IOPscience iopscience.iop.org

Home Search Collections Journals About Contact us My IOPscience

Silicon photonics beyond silicon-on-insulator

This content has been downloaded from IOPscience. Please scroll down to see the full text.

2017 J. Opt. 19 053001

(http://iopscience.iop.org/2040-8986/19/5/053001)

View the table of contents for this issue, or go to the journal homepage for more

Download details:

IP Address: 132.170.212.14
This content was downloaded on 04/04/2017 at 20:29

Please note that terms and conditions apply.

IOP Publishing Journal of Optics
J. Opt. 19 (2017) 053001 (13pp) https://doi.org/10.1088/2040-8986/aa5f5e

Topical Review

# Silicon photonics beyond silicon-on-insulator

**Jeff Chiles**[1,3] **and Sasan Fathpour**[1,2,4]

[1] CREOL, The College of Optics and Photonics, University of Central Florida, Orlando, FL, United States of America
[2] Department of Electrical Engineering, University of Central Florida, Orlando, FL, United States of America

E-mail: fathpour@creol.ucf.edu

Received 16 November 2016, revised 12 January 2017
Accepted for publication 9 February 2017
Published 4 April 2017


**Abstract**

The standard platform for silicon photonics has been ridge or channel waveguides fabricated on silicon-on-insulator (SOI) wafers. SOI waveguides are so versatile and the technology built around it is so mature and popular that silicon photonics is almost regarded as synonymous with SOI photonics. However, due to several shortcomings of SOI photonics, novel platforms have been recently emerging. The shortcomings could be categorized into two sets: (a) those due to using silicon as the waveguide core material; and (b) those due to using silicon dioxide as the bottom cladding layer. Several heterogeneous platforms have been developed to address the first set of shortcomings. In such important heterogeneous integrated photonic platforms, the top silicon layer of SOI is typically replaced by a thin film of another optical material with a refractive index higher than the buried oxide (BOX) bottom cladding layer. Silicon is still usually preferred as the substrate of choice, but silicon has no optical functionality. In contrast, the second category of solutions aim at using silicon as the core waveguide material, while resolving issues related to the BOX layer. Particularly, one of the main drawbacks of SOI is that the BOX layer induces high optical loss in the mid-wavelength infrared (mid-IR) range. Accordingly, a host of platforms have been proposed, and some have been demonstrated, in which the BOX is replaced with insulating materials that have low intrinsic loss in the mid-IR. Examples are sapphire, lithium niobate, silicon nitride and air (suspended Si membrane waveguides). Although silicon is still the preferred substrate, sometimes a thin film of silicon, on which the optical waveguide is formed, is directly placed on top of another substrate (e.g., sapphire or lithium niobate). These alternative substrates act as both mechanical support and the lower cladding layer. In addition to the demands of mid-IR photonics, the non-SOI platforms can potentially offer other advantages and flexibilities. Examples are different, and sometimes interesting, guided mode properties (e.g., single-mode and single-polarization behavior), enhanced dispersion engineering (wideband anomalous regimes), as well as ease of fabrication and higher thermal conductivity in some cases. The objective of this article is to review this category of non-SOI photonic platforms that use silicon as the waveguide core layer and discuss their challenges and opportunities.

Keywords: silicon photonics, mid-infrared photonics, suspended membrane waveguides, heterogeneous integration

(Some figures may appear in colour only in the online journal)

[3] Now at the National Institute of Standards and Technology (NIST), Boulder, CO, United States of America.
[4] Author to whom any correspondence should be addressed.

 © 2017 IOP Publishing Ltd Printed in the UK

## 1. Introduction

Silicon photonics has advanced dramatically since its inception in the 1980s [1, 2]. For the most part, this path of technological development was motivated by the prospect of leveraging the significant advancements in the maturity of fabrication processes developed for the electronics industry [3]. A significant aspect of this was the availability of inexpensive and extremely high-quality silicon substrates. Early implementations of silicon photonic waveguides relied on the low index contrast provided by material doping to form a waveguide core [1]. But soon afterward, a new technology enabled a completely new approach and incredible performance improvements. This was the introduction of silicon-on-insulator (SOI) wafers [4]. The high index contrast afforded by this technology enabled the sophistication of silicon photonics to grow rapidly [5–8]. Since then, silicon photonics has reached sufficient maturity for commercial telecommunications applications at significant production volumes [9, 10].

However, silicon has well-known shortcomings in terms of light detection (in the telecommunication band) and light generation at any band [1]. It also lacks second-order optical nonlinearity and suffers from nonlinear absorptions when its third-order optical nonlinearity is exploited [2]. This has motivated heterogeneous integration of other materials ranging from III–V compound semiconductors, germanium, second- and third-order nonlinear optical material (e.g., lithium niobate, aluminum nitride, silicon nitride, high-index nonlinear glasses or metallic oxides) on silicon substrates. The main feature in these approaches is that Si is abandoned as the waveguide core material and replaced with another suitable material for a specific optical functionality. Among others, these approaches have been a main direction in our team's research [11–18]. These works, as well as related those by other groups, are reviewed recently elsewhere [19], and hence are not the focus of this paper. Rather, the objective is to review non-SOI devices and platforms, developed by us and others, that use Si as the core waveguide material, albeit sometimes on non-Si substrates, as motivated in the following.

Just as the electronics industry seeded its initial development, silicon photonics for telecommunications may now jump-start the development of related technology for completely different applications. It has long been established that crystalline silicon exhibits a broad transparency window spanning the mid-wavelength infrared (mid-IR) region of 3–8 $\mu$m, making it highly valuable for integrated photonics [20, 21]. This important spectral region is crucial to many fields and technologies. Free-space communications [22] stand to benefit greatly from superior immunity to turbulence when implemented at longer wavelengths [23]. Hyperspectral imaging conducted in this spectral region could allow enhanced orbital environmental monitoring [24]. Dual-comb mid-IR spectroscopy could allow the rapid identification of airborne contaminants with extreme precision [25]. To date, solutions to these challenges (capable of mid-IR operation) have been primarily implemented in bulky free-space optical setups with little hope of evolving into field-worthy systems. It is for this reason that silicon photonics, with decades of work put into the design and fabrication of ultracompact optical devices, has become a prime candidate for mid-IR integrated photonics.

However, silicon is not the only material under investigation for mid-IR integrated photonics. It could be argued that the earlier mentioned applications, while important, will likely never demand the volume that justified the efforts dedicated to integrated telecommunications products. If only thousands of units may be needed over a timescale of years, it makes little difference whether the integrated photonic chip is a few dollars or hundreds of dollars, depending on the complexity of the entire system. Thus, the benefits of other material platforms must be fairly considered with a diminished emphasis on their overall cost, or worthiness for high-volume production.

Nonetheless, silicon has several key advantages, which collectively set it apart from the aforementioned alternative platforms that heterogeneously integrate other materials on silicon substrates, e.g., chalcogenide glass, silicon nitride and semiconductors [26–29]. Namely, it allows high-index contrast thanks to the ease of patterning and etching silicon waveguides; it is highly stable as a monocrystalline material with excellent thermal and mechanical properties; its refractive index can be guaranteed to an extraordinary precision thanks to mature substrate fabrication; it offers a transparency window bridging the near-to-mid-IR with no absorption peaks interrupting it; and it can be directly integrated with electronics. It should be noted that while amorphous silicon has been considered for mid-IR applications [30] and potentially has benefits thanks to its low-cost substrate preparation, the intrinsic absorption due to hydrogen content drastically limits its transparency window [31]. Furthermore, it has been shown to exhibit instabilities over time [32], a severe limitation. Thus, it is clear that crystalline silicon stands above many alternatives in this application space.

However, SOI is not an ideal platform for mid-IR integrated photonics. Its buried oxide (BOX) layer exhibits strong absorption at 3 $\mu$m and above 4 $\mu$m [33]. While it served well for initial investigations of nonlinear photonics in silicon in the mid-IR [34–37], as well as integrated detector technology in the $\sim$2 $\mu$m wavelength range [38, 39] it does not provide a complete solution for the first atmospheric transmission window, which spans 3–5 $\mu$m. If the thickness of the silicon device layer is increased to avoid overlap into the lossy silicon dioxide at longer wavelengths, it begins to compromise the overall compactness of the system. This has motivated the exploration of alternative platforms for monocrystalline silicon photonics that avoid the use of the BOX layer, in order to maximize their transparency. It is noted that silicon-on-silicon [40, 41] is in principle an alternative to SOI suitable for mid-IR applications. Indeed, doping silicon to create index contrast for vertical optical confinement is the original proposed silicon photonics platform predating SOI [1]. However, the very low vertical index contrast of the waveguides and the free-carrier loss associated with doping silicon renders silicon-on-silicon less attractive. In this work, we review and discuss several other promising high-contrast platforms, each

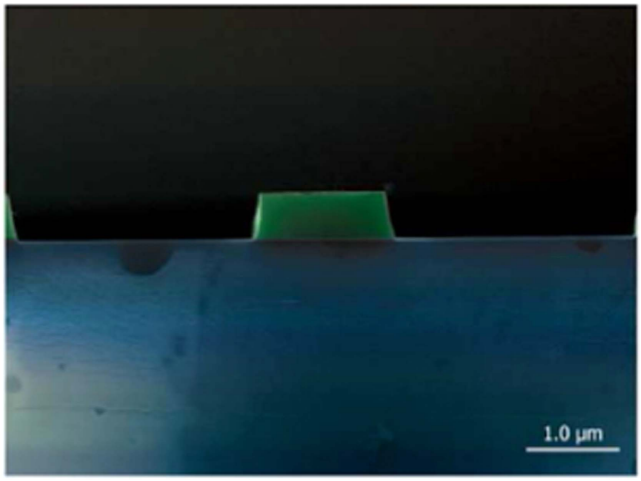


**Figure 1.** Cleaved facet of a silicon-on-sapphire waveguide. Figure reproduced from [45]. © The Optical Society.

with unique advantages and targeted applications. Some of them were proposed as early as a decade ago [20, 21], and demonstrated later by various researchers, while some were proposed and demonstrated later.

## 2. Silicon on sapphire

Sapphire substrates have been long used for silicon-based electronics thanks to their insulating properties and radiation-hardened operation [42]. This platform, known as silicon-on-sapphire (SOS), takes advantage of the lattice-matching between silicon and sapphire that is possible for R-plane-oriented sapphire substrates [43], which enables epitaxial growth of crystalline silicon through chemical vapor deposition. Sapphire also exhibits transparency from the visible to roughly 5 $\mu$m [44], enabling it to be used for mid-IR applications concerning the first atmospheric transmission window. SOS substrates are commercially available at relatively low costs, even for low volume purchases. Of course, compared to SOI, SOS does not compete in its cost or volume of manufacturing. But the fact that these finished substrates can be purchased even in a single-unit quantity makes them highly attractive for laboratory studies, which is indeed the first step to demonstrating their feasibility for more advanced projects. Furthermore, their processing is largely similar to that of SOI, allowing them to be investigated without extensive re-tooling of facilities or processes. As will be seen in later sections of this review, several other silicon-based platforms are available with some advantages over SOS, although they require substantial post-processing or substrate preparation. Thus, SOS will likely stand on its own for some time in the domain of shorter-wavelength studies in the mid-IR.

The first experimental demonstration of SOS photonics in the mid-IR was by Baehr-Jones *et al* in 2010 [45]. In this work, SOS channel waveguides were dry etched via $CF_4$ plasma (figure 1). Several lengths of waveguides were prepared on a chip, and then tested via the cut-back method with an optical parametric oscillator (OPO). Propagation losses of 4.3 dB cm$^{-1}$ for the transverse-electric (TE) mode were recorded at a wavelength of 4.5 $\mu$m, demonstrating that epitaxially grown films on these substrates could be patterned and used for high-quality optical waveguides at long wavelengths. A minimum bending radius of 40 $\mu$m was employed for the cut-back waveguide layouts, and coupling losses on-and-off-chip were estimated to be 18 dB/facet, employing single-mode fibers at the input and output. The same research group also demonstrated ring-resonators operating at 5.4–5.6 $\mu$m with $Q$-factors of 3000 [46]. Other devices on the SOS platform were demonstrated by Zou *et al* including fiber-to-waveguide grating couplers with 29% coupling efficiency for the TE polarization [47] at 3.4 $\mu$m wavelength, and photonic crystal cavities with a quality factor of 3500 at a wavelength of 3.43 $\mu$m [48].

Improved waveguiding performance on SOS was demonstrated in 2013 by Shankar *et al* [49]. The waveguides were patterned with pseudo-Bosch etch chemistry, and their propagation losses were improved through post-processing with several chemical oxidation treatments. This led to high-quality ring resonators (radius = 60 $\mu$m) with intrinsic quality factors of 278 000 (figure 2(b)), and a corresponding propagation loss of 0.74 dB cm$^{-1}$ for the TE-mode at $\lambda = 4.5$ $\mu$m. Grating couplers on the input side were fabricated, with an estimated coupling efficiency of 40%. Coupling losses were estimated to be 6 dB on the output side using horn-shaped output tapers. However, experimental characterization of these efficiencies was not performed in this work. A proof-of-concept demonstration in gas sensing using SOS ring-resonators was demonstrated by the same group in 2015, showing a sensitivity of 5000 ppmv for $N_2O$ [50]. In the scope of nonlinear optics, supercontinuum generation in SOS waveguides, spanning from 2 to 6 $\mu$m, was later demonstrated in 2015 by Singh *et al* [51], based on ridge waveguides pumped by a femtosecond laser source. SOS has shown to be a versatile platform enabling a rich variety of photonic devices, and thanks to its affordability and availability, it will likely continue to expand in the coming years for integrated photonics in the 3–5 $\mu$m spectrum.

## 3. Suspended membranes on SOI

Despite the advantages of SOS, it still has several shortcomings limiting its utility in other integrated photonics applications. The most significant limitation is its limited transparency based on sapphire absorption [44]. Depending on the thickness of silicon used, it may achieve low-loss operation into the low 5 $\mu$m range, but it cannot easily be pushed further. This has driven the pursuit of silicon photonic platforms, in which the waveguide solely interacts with air-clad silicon. In this section, we discuss the development and application of suspended silicon waveguides built on SOI substrates.

SOI substrates have been previously used as a platform for suspended photonics, though primarily for studies of photonic crystal structures operation at near-IR wavelengths

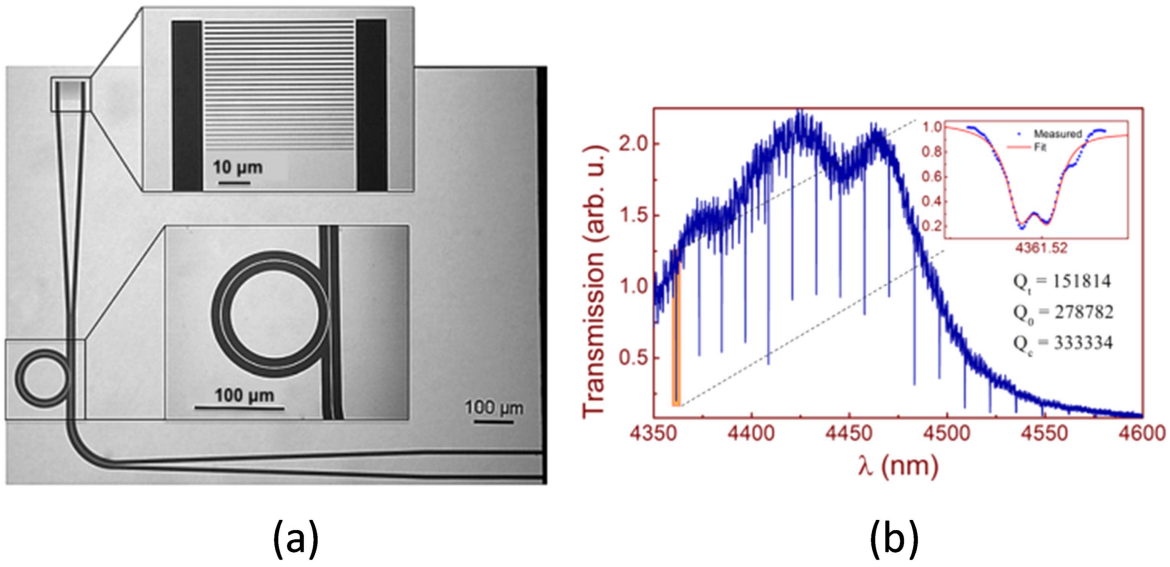


**Figure 2.** (a) Optical micrograph of a fabricated SOS micro-ring resonator and grating coupler; (b) transmission spectrum of a ring resonator, showing high-quality-factor resonances in the mid-IR. Reprinted with permission from [49]. Copyright (2017), AIP Publishing LLC.

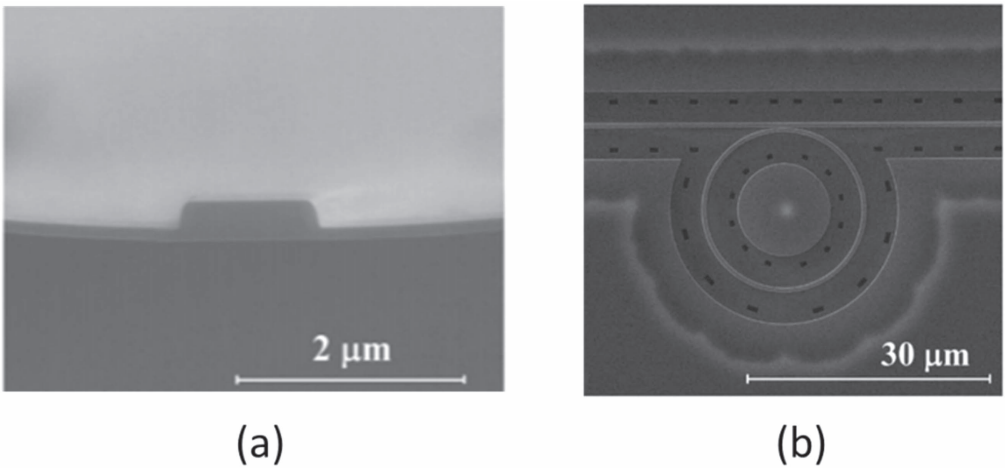


**Figure 3.** Scanning electron micrographs of suspended ridge-type structures after undercut etching; (a) cross section of a waveguide facet; (b) top-view of a ring resonator. Figures reproduced with permission from [54]. © (2017) IEEE.

[52, 53]. All such structures are formed by the puncture of the device-layer silicon and a subsequent liquid (or vapor-phase) etch of the BOX layer, forming a suspended silicon membrane. By submersing the structure in etchant for longer periods of time, the extent of the undercut can be controlled, depending on the size of the structure required.

### *3.1. Suspended ridge waveguides on SOI*

Suspended SOI membrane waveguides specifically designed for mid-IR operation were first experimentally demonstrated by Cheng *et al* in 2012 [54], by a two-step process. In the first step, a ridge waveguide structure was formed by etching a blank SOI wafer. In the second step, a periodic series of holes were etched into the vicinity of the ridges. The membranes were released by a timed liquid etch of the BOX layer, forming a roughly $\sim$18 $\mu$m wide suspended slab region (figure 3). Cut-back measurements were performed for various waveguide lengths, showing TE-mode losses as low as $3.0 \pm 0.7$ dB cm$^{-1}$ at a wavelength of 2.75 $\mu$m. Light was coupled on and off-chip with grating couplers and single-mode fibers. Waveguide bends with radii of 40 $\mu$m were employed. Racetrack resonators were also fabricated and characterized in the mid-IR, showing a $Q$ value of 8100 via thermal tuning through its resonance. Later, focusing sub-wavelength grating couplers were demonstrated on this platform by the same group, achieving 24.7% coupling efficiency for the TE polarization at $\lambda = 2.75$ $\mu$m [55], as well as graphene-based photodetectors operating at 2.75 $\mu$m [56]. Elsewhere, suspended ridge-type ring resonators were demonstrated at longer wavelengths of 3.4 and 5.2 $\mu$m by Xia *et al* [57]. Improved quality factors of up to 83 000 at $\lambda = 3.79$ $\mu$m were recently demonstrated by Miller *et al* [58], through etchless waveguide processing, as well as nanotaper couplers on- and off-chip with a coupling loss of 6–7 dB/facet.

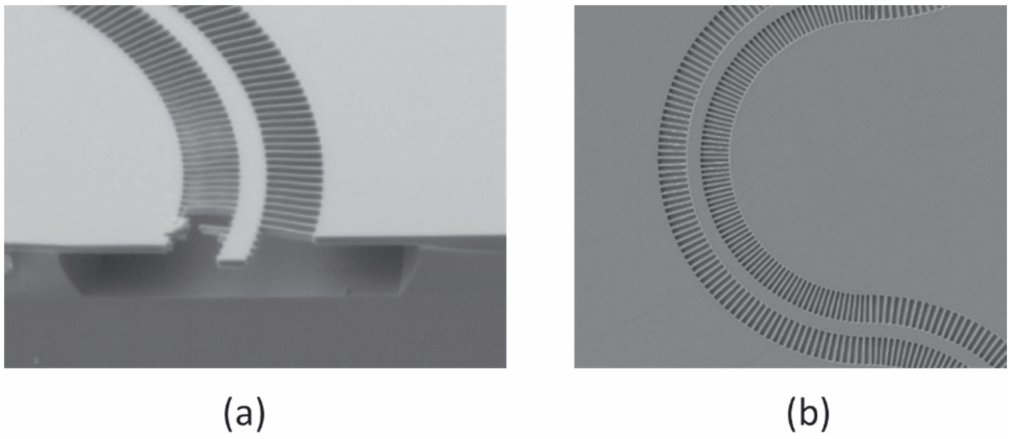


**Figure 4.** Scanning electron micrographs of suspended metamaterial waveguide structures after undercut etching; (a) cross section of a waveguide facet; (b) top-view of a bent waveguide. Figures reproduced from [60]. © The Optical Society.

An in-depth mechanical analysis of the tradeoffs involved in parameters such as silicon thickness, etch depth and hole dimensions was performed to assess the prospects of suspended ridge membrane waveguides [54]. Ultimately, the surface perforations, combined with the wide suspended regions, are responsible for introducing significant strain in the silicon structure, constraining it to modest etch depths before damage may occur. Nevertheless, this approach is meritable for several reasons, such as its use of a commonly available substrate, relatively simple fabrication, and that its intrinsic geometry does permit most conventional silicon photonic structures to be readily fabricated.

### *3.2. Sub-wavelength grating waveguides on SOI*

An alternative approach to suspended SOI waveguides was proposed and demonstrated in 2014 by Soler Penadés *et al* [59]. In contrast to the previously described suspended-ridge geometry [54], this instead utilized surface perforations to simultaneously provide lateral optical confinement, as well as access for undercut etching, simplifying the lithography to one step. It was implemented as a series of rectangular holes of sub-wavelength dimensions on either side of an unetched silicon slab comprising the waveguide core (figure 4). At mid-IR wavelengths, the silicon struts supporting the waveguide could be made small enough to have a diminished scattering effect. Initially, a propagation loss of 3.4 dB $cm^{-1}$ for the TE-mode was achieved at a wavelength of 3.8 $\mu$m, with a sub-wavelength grating period of 300 nm. This structure was later improved upon [60] by widening the core from 1.1 to 1.3 $\mu$m, improving the isolation of the mode from the cladding structure, and by using a 4 nm electron-beam spot size compared to 20 nm in the previous work; these improvements led to reduced propagation losses of 0.82 dB $cm^{-1}$ at 3.8 $\mu$m wavelength. Coupling on and off-chip was done by grating couplers. Additionally, several important integrated photonic elements were demonstrated on this platform, such as low-loss bends with radii of 15.7 $\mu$m, and a 2 $\times$ 2 multi-mode interferometer with a power imbalance of 0.5 dB and excess loss of 1.6 dB. These were also incorporated into an asymmetric Mach–Zehnder interferometer (MZI), showing a minimum extinction ratio of 15 dB. These promising results show that sub-wavelength grating-based suspended silicon photonics are capable of some essential building blocks for effective performance in the mid-IR. However, as with the previously discussed ridge-type suspended SOI membranes, these structures exhibit mechanical sensitivity introduced by the use of etch-holes. Although the width of the suspended region is significantly narrower in this case, the extent of the surface perforation is much greater compared to ridge-type membranes. Indeed, the structures of [60] incorporated reduced cladding widths of 2.5 $\mu$m compared to the prior cladding width of 4 $\mu$m in [59], in order to mitigate this. Furthermore, in order to operate out to the transparency limit of 8 $\mu$m as proposed, significantly wider core and cladding dimensions (and concomitant reduced stability) may be required to mitigate lateral leakage loss. Further studies may elucidate the necessary design choices in this matter.

## 4. All-silicon optical waveguides

The previous section discussed recent progress on the development of suspended silicon waveguiding structures built on SOI substrates. A necessary element in their implementation is the use of access holes and undercut etching to remove the BOX layer underneath. Effectively, this imposes significant design constraints on the geometries employed, in terms of balancing their mechanical stability with choices such as lateral cladding dimensions or lower air gap thickness. Additionally, the necessity of a thick BOX layer on the SOI substrate inhibits good thermal conduction from the device layer to the substrate. In this section, we discuss the development of another branch of photonic waveguiding structures that are implemented on *all-silicon* platforms, which mitigate some of these issues and achieve superior mechanical stability.

### *4.1. Suspended-membrane ASOP*

The suspended ridge waveguide geometry discussed earlier was seen to have the advantage of generally good compatibility with conventional silicon photonics devices [54], at the

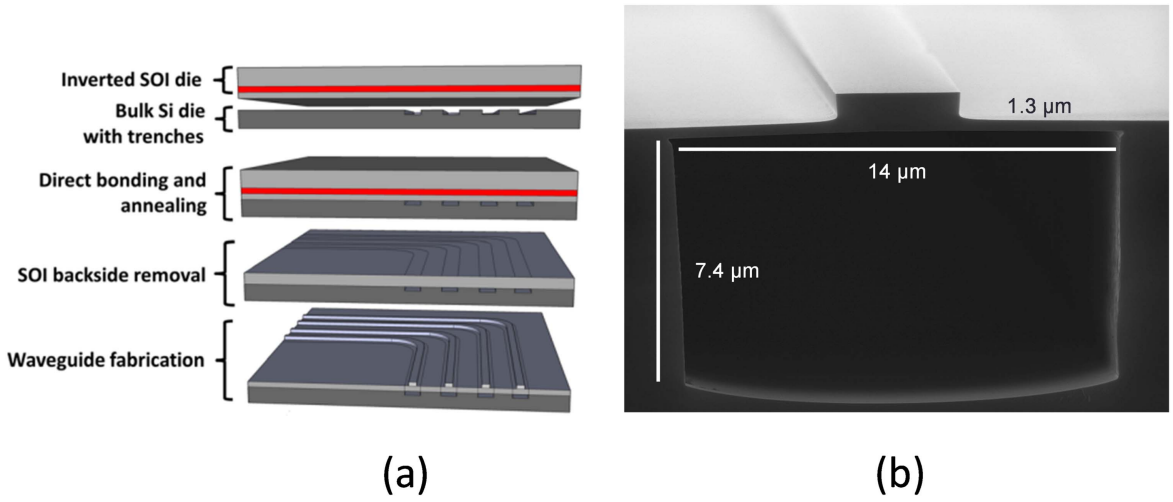


**Figure 5.** (a) ASOP fabrication process; (b) cleaved facet of an ASOP suspended-membrane waveguide. Figure reproduced from [62]. Copyright (2017), AIP Publishing LLC.

expense of limited mechanical stability from the wide exposed membrane structures and etch-holes which introduce strain. All-silicon suspended waveguides with ridge-like structures have been demonstrated using alternating passivation and etching on bulk silicon substrates [61], though they possess a strong interaction with roughly etched surfaces and etch-holes used in the process, and are not compatible with dense integration or most conventional photonic waveguide structures. In 2013, we demonstrated a novel suspended ridge geometry, deemed the all-silicon optical platform (ASOP), which effectively addresses the practical issues of other suspended silicon waveguiding platforms [62]. The suspended-membrane ASOP waveguides are formed in a wafer-bonding process as shown in figure 5(a). First, a handle die is etched with trenches wherever waveguides or devices are desired. Next, it is bonded to an inverted SOI die. Afterwards, the SOI die backside and BOX layer are removed, leaving a suspended silicon membrane on the handle die, over the trenches. Finally, ridge waveguides are patterned and etched on the handle die, forming the completed substrate (figure 5(b)). Since there is no need for undercut etching, the width of the suspended membrane can be determined entirely by the optical leakage requirements, improving its stability. This is further enhanced over other approaches, thanks to the absence of strain-inducing access holes. Also, the silicon membrane achieves a direct connection to the silicon substrate, enhancing its thermal conductivity over SOI-based approaches.

We have fabricated ASOP waveguides [62] starting with SOI wafers with a device layer thickness of $\sim$2.1 $\mu$m. Trenches with widths of 17 $\mu$m and a depth of 2 $\mu$m were used on the handle die. After bonding and backside removal, 2.4 $\mu$m wide ridge waveguides were patterned with contact lithography and etched to a thickness of $\sim$1.1 $\mu$m. Devices 5–7 mm in length were tested with Fabry–Perot measurements as the temperature of the sample was tuned, at a wavelength of 3.39 $\mu$m. Light was coupled in through polished facets without tapers on the input and output, using a single-mode fiber at the input and a multimode fiber at the output. The fundamental transverse-magnetic (TM) mode showed propagation losses of $2.8 \pm 0.5$ dB cm$^{-1}$, mainly limited by optical-lithography-induced defects, which could be remedied with electron-beam lithography or non-contact stepper lithography. The TE-mode showed somewhat higher losses of $4.0 \pm 1$ dB cm$^{-1}$. Overall, ASOP shows superior potential for scaling to longer wavelengths, thanks to its enhanced stability enabling wider membranes without compromising stability. It also supports the vast majority of conventional photonic device designs without adaptation. The only price that is paid for the advantages of ASOP is the need for a wafer-bonding and backside-removal step in the process. However, given the limited volume that is likely of interest to mid-IR integrated photonics, the added cost is not significant. Furthermore, the yield of fusion bonding processes is as of the date exceedingly good. A case in point of this is the low cost of commercially available SOI substrates, which themselves depend upon fusion bonding. It should also be noted that the critical surface area for ASOP structures, which is the portion underneath the suspended membrane, never contacts the handle wafer, significantly relaxing the constraints on wafer cleanliness in this case. Work is underway in bringing ASOP technology to the wafer scale, which will enable more advanced photonic devices to be readily demonstrated.

### *4.2. Anchored-membrane ASOP or T-Guides*

We recently demonstrated another novel ASOP-based waveguiding platform that realized anchored-membrane waveguides, or *T*-Guides [63] (figure 6). These structures, like the suspended-membrane ASOP, are achieved through a wafer-bonding process between and SOI and a pre-etched handle substrate. However, instead of patterning the waveguides after the bonding, *T*-Guides are formed as soon as the wafers are bonded. This is because the trench features on the handle substrate contain a small 'post' of silicon in the middle, which acts as a guiding defect for the waveguide mode once it is adjoined with the silicon membrane donated from the SOI substrate. This provides an even simpler fabrication

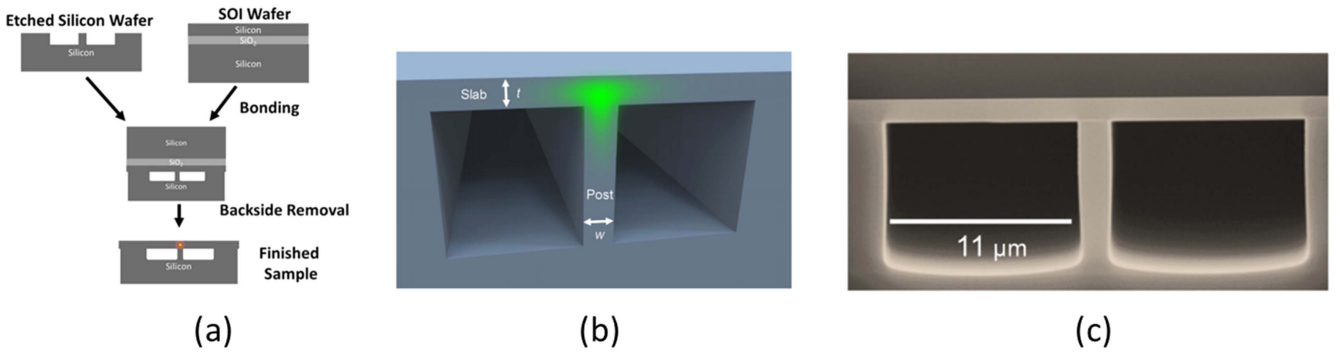


**Figure 6.** (a) Fabrication process for making silicon *T*-Guides; (b) schematic representation of the essential *T*-Guide geometry; (c) scanning electron micrograph of the cross section of a fabricated silicon-based *T*-Guide. Figures reproduced from [64] and [63]. © The Optical Society.

process than ASOP, since only one lithography step is required and the waveguide is always self-aligned to the center of the trench. It also has the advantage that the post simultaneously serves to further enhance the mechanical stability and thermal conductivity of the membrane and reduce the extent of the overhang required. This robust platform represents a valuable path of exploration for mid-IR integrated photonics given these advantages. To test this, we fabricated silicon-based *T*-Guides (figure 6(c)) based on a post width of 1.8 $\mu$m and a slab thickness of 1.3 $\mu$m [63]. The post/trench etch was achieved by pseudo-Bosch etch chemistry, allowing highly vertical features to be preserved in the post. The fabricated *T*-Guides were 5 cm long, and were measured at this length and at 2 cm for cut-back measurements, showing minimum TE mode propagation losses of $1.75 \pm 0.3\,\mathrm{dB\,cm^{-1}}$ at a mid-IR wavelength of 3.64 $\mu$m. Light was coupled on-chip via a lens with a high numerical aperture at the input and a single-mode fiber at the output, with cleaved facets on both sides of the chip. The propagation loss could be lowered even further, since the fabricated sample contained a small oxide layer on the inside of the trenches from the annealing, and the BOX layer was kept on top during testing to protect the sample during cleaving; both of these add some absorption loss which could be easily mitigated in the future for all-silicon devices.

We have also explored other interesting features of the *T*-Guide geometry, both theoretically and experimentally [63, 65]. These structures were found to exhibit wide-band single-mode and single-polarization (SMSP) operation, with silicon-based structures exhibiting a theoretical SMSP window of up to 2.75 octaves. This is shown in figure 7. This behavior is derived from their semi-infinite (from the direct connections to the substrate in both the post and slab dimensions) and asymmetric (*T*-shape) geometry. In effect, at most one transverse optical mode can experience the local effective index increase that leads to waveguiding at the junction of the post and slab. This immunity to higher-order modes makes them promising for integrated photonics applications where the beam quality must be maximized for eventual free-space propagation. Furthermore, the asymmetry of the structure generally forces the TM mode into cutoff, except for narrow-post geometries at short wavelengths,

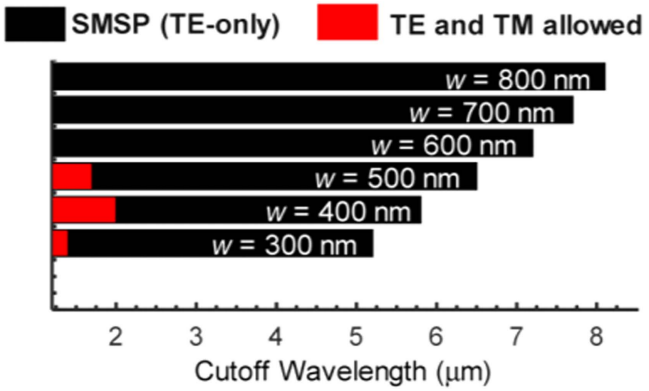


**Figure 7.** Single-mode and single-polarization window simulated for silicon-based *T*-Guides with fixed $t = 500$ nm, and varying post width. The black region indicates one transverse mode and only the TE polarization being supported, and the red region indicates the supported propagation of TM-polarized light. Figure reproduced from [63]. © The Optical Society.

meaning these waveguides naturally enforce highly polarized outputs. One disadvantage of *T*-Guides worth noting is that they are not compatible with the full range of conventional photonic devices, since excessively wide posts can result in substrate leakage. Additionally, since they cannot support multiple transverse modes, multimode interferometers are naturally out of the question. Therefore, they may find the most value when applied to fields such as nonlinear integrated photonics where waveguiding performance and modal management may be more pressing than dense integration. Finally, it is also interesting to note that the *T*-Guides or anchored-membrane ASOP structures can be readily co-integrated with the suspended-membrane counterparts, simply by modifying the handle substrate to include posts before bonding, allowing the advantages of both platforms to be blended.

### *4.3. Pedestal waveguides*

All-silicon waveguides for mid-IR operation can also be fabricated without any suspended membranes. A novel

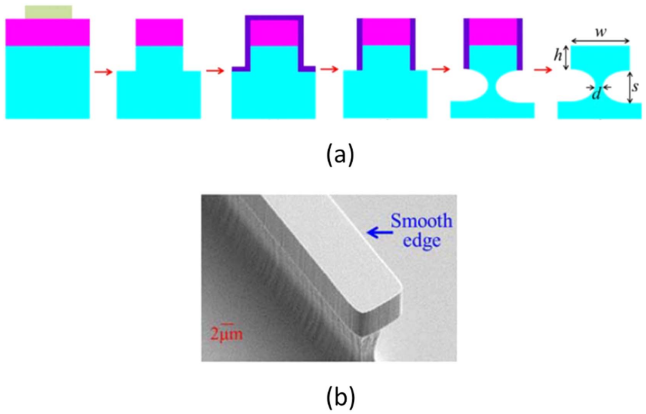


**Figure 8.** (a) Fabrication flow for pedestal-type waveguides, showing patterning, etching, conformal $SiO_2$ coating, anisotropic $SiO_2$ etching, isotropic Si etching, and removal of $SiO_2$ to produce the final structure; (b) scanning electron micrograph of a fabricated pedestal waveguide. Figures reproduced from [68]. © The Optical Society.

method for fabricating optical waveguides on bulk silicon substrates was demonstrated in 2013 by Chang *et al* with loss measurements conducted in the near-infrared [66, 67]. Lin *et al* [68] shortly after employed a similar method for fabricating pedestal-shaped silicon waveguides on bulk silicon substrates, with the purpose of utilizing them for the mid-infrared. The fabrication method consists of an initial, shallow silicon etch, followed by cladding deposition and directional etching to expose the silicon on the substrate. Next, an isotropic silicon etch ($SF_6$ chemistry) is used to undercut the silicon substrate underneath the protected waveguide core. Once a sufficient etch depth for optical isolation has been achieved, the oxide cladding is removed, resulting in a typical structure such as that shown in figure 8(b). Perhaps the most valuable practical advantage of this approach is that it only requires one inexpensive bulk silicon substrate, rather than specialized SOI wafers. Similar to the discussed *T*-Guide approach, it also exhibits superior thermal properties compared to those built on SOI. An all air-clad pedestal structure was tested between $\lambda = 2.5$–$3.7\,\mu$m, showing only fundamental-mode propagation, and a propagation loss of $2.7\,\mathrm{dB\,cm^{-1}}$ for the TE mode at $3.7\,\mu$m through paper-clip structures with a bending radius of $50\,\mu$m. Additionally, 50:50 *Y*-branch waveguide splitters were fabricated and measured, showing even splitting. Light was coupled on and off-chip via single-mode fibers aligned to cleaved waveguide facets. These pedestal waveguides were also used to perform on-chip liquid sensing of hexane and toluene through evanescent field interaction outside the waveguide core [69]. Pedestal waveguides offer an economical and prototyping-ready platform for mid-IR integrated photonics thanks to their relaxed substrate and substrate-preparation requirements. However, one notable limitation is that they are not readily compatible with many conventional integrated photonic structures, since the pedestal cannot be very narrow, nor very wide, without collapsing or introducing excessive substrate leakage through the base.

## 5. Mid-IR silicon photonics on novel substrates

So far, we have reviewed progress on mid-IR silicon photonic platforms based on sapphire, suspended SOI, or bulk silicon substrates. These approaches rely on commonly available substrates modified to suit a specific purpose, or well-established bonding procedures between silicon substrates. Another class of mid-IR platforms, which we will discuss in this section, instead seeks to replace the BOX lower cladding with more broadly transparent media. Thus, highly stable and general-purpose substrates can be manufactured, but still allow propagation at longer wavelengths than is practical with SOS substrates.

### 5.1. Silicon on nitride (SON)

One promising alternative to silicon dioxide for the lower cladding layer is silicon nitride, transparent up to $6.7\,\mu$m wavelength. This represents the SON platform, previously proposed and theoretically investigated in [20, 21, 70]. The relatively low refractive index of silicon nitride of $\sim$2 permits strong confinement to be retained on this platform, a necessity for practical operation at longer wavelengths. Our team provided the first experimental demonstration of mid-IR waveguiding on the SON platform [71]. The SON substrates were prepared by deposition of silicon nitride on an SOI substrate, followed by spin-on-glass-assisted bonding between silicon dioxide layers 'below' the silicon nitride and out of the reach of the optical mode; this process is depicted in figure 9(a). After backside removal, the silicon device layer rests atop the buried silicon nitride. Ridge waveguides approximately $2.0\,\mu$m wide were measured via Fabry–Perot oscillations (the same method as in [62]), showing minimum TM-mode propagation losses of $5.1 \pm 0.6\,\mathrm{dB\,cm^{-1}}$ were observed at a measurement wavelength of $3.39\,\mu$m. The TE-mode showed losses of $5.2 \pm 0.6\,\mathrm{dB\,cm^{-1}}$. The coupling method was identical to that used in [62].

The SON platform has since been used for the integration of quantum-cascade lasers (QCLs) on silicon substrates in 2016 by Spott *et al* [72]. The active region was evanescently coupled to an SON waveguide underneath, with transitions to passive silicon waveguides outside the active region. The Fabry–Perot lasing cavity was formed by polished, uncoated facets. A single-sided output power of up to 31 mW was observed in pulsed-operation mode at room temperature, at a mid-IR emission wavelength of $4.8\,\mu$m. This same integration approach was also used to demonstrate distributed-feedback QCLs by etching gratings into the silicon waveguides of the devices, which were capable of pulsed emission of >200 mW at wavelengths from 4.6 to $4.9\,\mu$m, although single-mode operation was not yet achieved [73]. These works demonstrate the broad applicability of the SON platform to advanced integration in mid-IR silicon photonics.

### 5.2. Silicon on lithium niobate (SiLN)

Crystalline silicon possesses inversion symmetry in its crystalline structure, which means it has no second-order optical

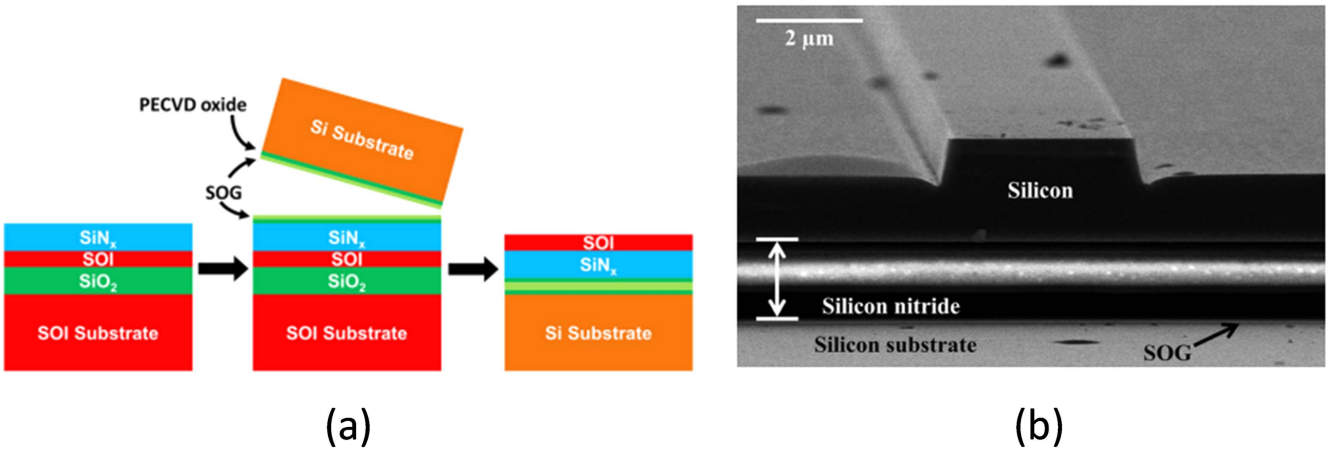


**Figure 9.** (a) Fabrication process for preparing SON substrates; (b) cross sectional view of a fabricated SON waveguide. Reprinted with permission from [71]. Copyright (2017), AIP Publishing LLC.

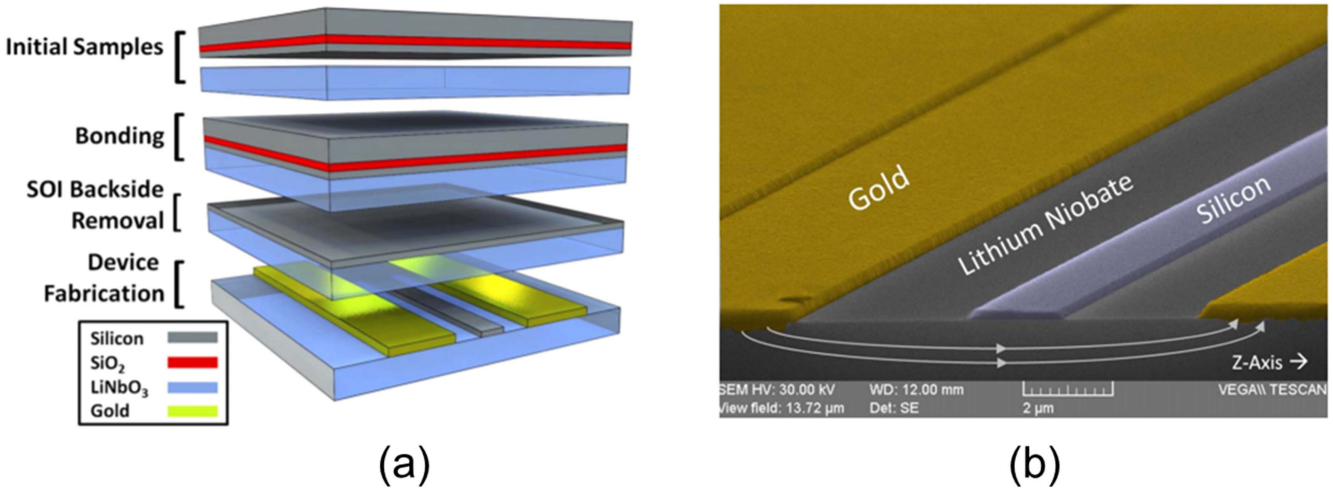


**Figure 10.** (a) Fabrication process for producing SiLN dies and electro-optic modulators; (b) cross-sectional and false-colored image of a SiLN modulator, showing the silicon waveguide surrounded by gold electrodes to establish an electric field through the lithium niobate substrate. Figures reproduced from [75]. © The Optical Society.

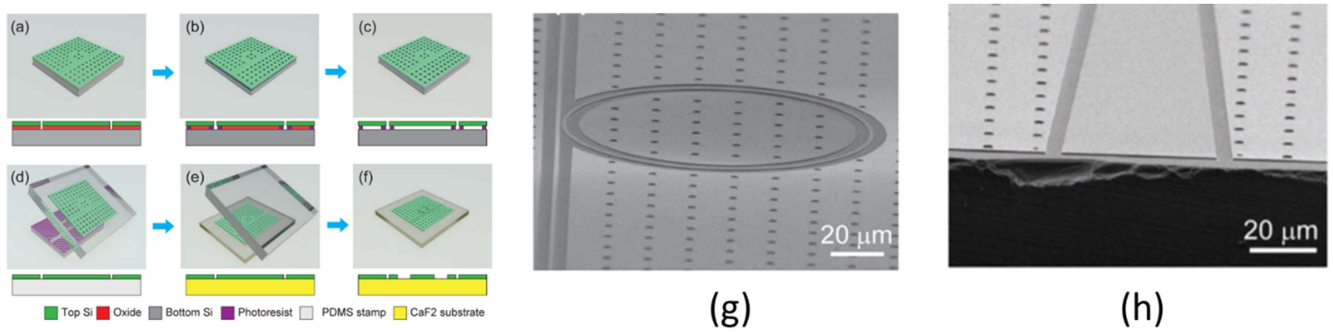


**Figure 11.** (a)–(f) Fabrication procedure for silicon on calcium fluoride photonic devices, showing the steps involved in transferring the membrane to the new substrate; (g) scanning electron micrograph of a silicon on calcium fluoride micro-ring resonator; (h) cross section of a chip facet. Figures reprinted with permission from [78]. Copyright (2014) American Chemical Society.

nonlinearity or Pockels effect. This limits its usage for active optical devices such as modulators. Although plasma dispersion-based modulators [1] have been highly successful for near-IR telecommunications-oriented silicon photonics, they have limited applicability in the mid-IR. One limitation is the quadratic increase in free-carrier absorption with increasing operational wavelength, which leads to significant absorption being coupled to phase changes induced by the free carriers [74]. This means that a pure phase modulator is not practical to achieve with this method at such long wavelengths. A

**Table 1.** Comparison of mid-IR integrated photonic platforms.

| Platform and relevant works | Advantages | Disadvantages | Lowest mid-IR propagation loss reported (dB $cm^{-1}$) |
|---|---|---|---|
| Silicon-on-sapphire (SOS) [45–51] | Commercially available substrates, low process complexity, mechanically supportive substrate | Hard substrate makes facet preparation more challenging, epitaxially grown silicon may have material-limited losses, limited transparency window | 0.74 [49] |
| Suspended ridge waveguides on SOI [54, 55, 57, 58] | Commercially available substrates, good compatibility with conventional photonic structures | Poor mechanical stability, additional etching step required | 3.0 [54] |
| Sub-wavelength grating waveguides on SOI [59, 60] | Compact structures, single-step self-aligned waveguide etching, commercially available substrates | Geometry somewhat constrained by stability considerations, transparency window limited by grating effect and lateral leakage | 0.8 [60] |
| Bonded membrane ridge waveguides (suspended-membrane ASOP) [62] | Compatible with almost all conventional photonic structures, flexible geometry choices, good mechanical stability | Requires in-house wafer bonding for every wafer processed, somewhat higher process complexity | 2.8 [62] |
| Anchored-membrane waveguides (*T*-Guides) [63, 65] | Wideband single-mode and single-polarization operation, self-aligned processing, can augment suspended-membrane ASOP approach, mechanically supportive substrate | Weaker lateral index contrast and lower optical confinement, requires wafer bonding, not compatible with all conventional photonic structures | 1.75 [63] |
| Pedestal waveguides [66, 68, 69] | Cheap and readily obtained substrates, strong optical confinement, mechanically supportive substrate | Poor geometrical design flexibility, poor compatibility with conventional photonic structures | 2.7 [68] |
| Silicon-on-nitride (SON) [20, 21, 70–72] | Wide transparency window, mechanically supportive substrate, good compatibility with conventional processing due to silicon substrate | Requires wafer bonding and additional substrate preparation steps, lack of commercially available substrates | 5.1 [71] |
| Silicon-on-lithium–niobate (SiLN) [75] | Multi-functional substrate enabling electro-optic and $\chi^{(2)}$ effects, mechanically supportive substrate | Limited transparency window similar to SOS, requires wafer bonding, lack of commercially available substrates | 2.5 [75] |
| Silicon on calcium fluoride [78] | Nearly perfect transparency window for Si, mechanically supportive substrate | Complex and non-scalable fabrication process, lack of commercially available substrates | 3.8 [78] |

means of solving this problem, and simultaneously broadening the transparency window available, is to transfer crystalline silicon membranes onto a lithium niobate substrate (SiLN), which we first experimentally demonstrated in 2014 [75]. Lithium niobate has been used successfully for decades in the production of high-bandwidth, high-extinction ratio optical modulators [76]. With its broad optical transparency into the mid-IR, it has also been used for mid-IR integrated OPOs with diffused waveguides [77]. SiLN allows the compactness, quality and stability of silicon waveguides to be combined with the electrooptical capabilities of lithium niobate. It is noteworthy that this SiLN heterogeneous approach for mid-IR applications, should not be confused with our other developed technology of thin-film lithium niobate on Si substrates, buffered by an oxide cladding layer, for near-IR electrooptic and nonlinear applications [12].

We demonstrated channel-type SiLN waveguides arranged into push–pull MZI electro-optical modulators driven by lateral electrodes (figure 10(b)) [75]. Integrated mid-IR modulators at a wavelength of 3.39 $\mu$m were demonstrated, showing on-chip insertion losses of 3.3 dB, an extinction ratio of 8 dB, TE-mode propagation losses of 2.5 $\pm$ 0.7 dB $cm^{-1}$, and a half-wave voltage product of 26 V cm. Light was coupled on and off chip via partially etched grating couplers, with a single-mode fiber at the input side and a multimode fiber on the output side. Although the maximum measured modulation frequency was 23 KHz (limited only by the detector response), these devices could be readily adapted to work at GHz speeds by optimizing the electrode configuration, thus providing a valuable means of achieving high-performance optical modulation in the mid-IR for applications such as free-space communication.

### 5.3. Silicon on calcium fluoride

Another mid-IR transparent substrate that has been investigated for silicon photonics, up to wavelengths of 8 $\mu$m, is calcium fluoride; this was first experimentally demonstrated in 2014 by Chen *et al* [78]. Unlike in the cases of ASOP, SON or SiLN, the silicon layer transfer was achieved by

peeling and pressing with a flexible temporary substrate. The silicon membrane was transferred in this way onto a final calcium fluoride substrate, with an area of 1.5 × 0.8 cm. Microring resonators with radii of 60 $\mu$m (figure 11(g)) were measured with a tunable QCL at 5.2 $\mu$m, showing propagation losses of 3.8 dB cm$^{-1}$ for the TE-mode, and a maximum intrinsic quality factor of 62 000. Light was coupled on and off-chip with inverse tapers and a single-mode fiber on the input, and lensed output coupling. To demonstrate the platform's applicability to on-chip, cavity-enhanced spectroscopy, the resonators were immersed in various cyclohexane solutions with ethanol, toluene, or isopropanol, showing good agreement with the predicted absorption spectra over the limited scanning range of the QCL source used in the experiment. This shows promising initial performance for crystalline silicon on calcium fluoride as a platform, although compatibility with wafer-scale processing is crucial to more extensive studies, and would require further work to optimize membrane transfer at these levels.

## 6. Conclusion

Crystalline silicon has proven a reliable choice for integrated photonic technology in the mid-IR spectral region in recent years, despite burgeoning efforts in many other material systems. Although SOI technology still plays a crucial role as a low-cost source of crystalline silicon membranes, the waveguide geometries have evolved into many varieties of suspended or anchored structures. Furthermore, the stability, high optical nonlinearity, ease of processing, and low cost of crystalline silicon have enabled it to succeed on many other substrates or bottom cladding layers, including sapphire, silicon nitride, lithium niobate and calcium fluoride, to accommodate broader wavelengths or advanced photonic functionality. The mid-IR platforms discussed in this work are summarized and compared in table 1.

It can be seen that most crystalline silicon mid-IR platforms demonstrated to date exhibit propagation losses roughly between 0.7 and 3 dB cm$^{-1}$. The performance is likely limited by sidewall roughness or lithography defects, given the lack of significant material absorption in high-quality crystalline silicon in the range of $\lambda = 2.8$–5 $\mu$m where most of these measurements were conducted. Although there are promising developments to date in basic photonic components on these platforms, dense integration and multi-functional systems yet remain on the horizon. Once the sophistication of telecommunications-sector photonic circuits can be transported to mid-IR silicon photonics, we may see quick payoffs in critical applications for this technology as size, weight and power benefits are realized.

## Funding

The works presented by this team here are being supported by the United States' Office of Naval Research (ONR) Young Investigator Program (YIP) under the Grant Number 11296285 and the National Science Foundation CAREER Program under Award Number ECCS-1150672.

## References

[1] Soref R and Larenzo J 1986 All-silicon active and passive guided-wave components for $\lambda = 1.3$ and 1.6 $\mu$m *IEEE J. Quantum Electron.* **22** 873–9
[2] Jalali B and Fathpour S 2006 Silicon photonics *J. Lightwave Technol.* **24** 4600–15
[3] Hochberg M and Baehr-Jones T 2010 Towards fabless silicon photonics *Nat. Photon.* **4** 492–4
[4] Lasky J B 1986 Wafer bonding for silicon-on-insulator technologies *Appl. Phys. Lett.* **48** 78–80
[5] Jalali B, Yegnanarayanan S and Trinh P D 1995 Integrated optical directional couplers in silicon-on-insulator *Electron. Lett.* **31** 2097–8
[6] Fischer U, Zinke T and Petermann K 1995 Integrated optical waveguide switches in SOI *1995 IEEE Int. SOI Conf. Proc.* (Piscataway, NJ: IEEE) pp 141–2
[7] Trinh P D, Yegnanarayanan S and Jalali B 1996 5 × 9 integrated optical star coupler in silicon-on-insulator technology *IEEE Photonics Technol. Lett.* **8** 794–6
[8] Jalali B, Yegnanarayanan S, Yoon T, Yoshimoto T, Rendina I and Coppinger F 1998 Advances in silicon-on-insulator optoelectronics *IEEE J. Sel. Top. Quantum Electron.* **4** 938–47
[9] Intel® silicon photonics 100G PSM4 optical transceiver brief (http://intel.com/content/us/en/architecture-and-technology/silicon-photonics/optical-transceiver-100g-psm4-qsfp28-brief.html)
[10] Luxtera ships one millionth silicon photonic transceiver product (http://luxtera.com/luxtera/Luxtera_1M_final_4.pdf)
[11] Chiles J, Malinowski M, Rao A, Novak S, Richardson K and Fathpour S 2015 Low-loss, submicron chalcogenide integrated photonics with chlorine plasma etching *Appl. Phys. Lett.* **106** 111110
[12] Rabiei P, Ma J, Khan S, Chiles J and Fathpour S 2013 Heterogeneous lithium niobate photonics on silicon substrates *Opt. Express* **21** 25573–81
[13] Rao A, Patil A, Chiles J, Malinowski M, Novak S, Richardson K, Rabiei P and Fathpour S 2015 Heterogeneous microring and Mach–Zehnder modulators based on lithium niobate and chalcogenide glasses on silicon *Opt. Express* **23** 22746
[14] Rao A, Patil A, Rabiei P, Honardoost A, Desalvo R, Paollela A and Fathpour S 2016 High-performance and linear thin-film lithium niobate Mach–Zehnder modulators on silicon up to 50 GHz *Opt. Lett.* **41** 5700–3
[15] Rao A, Malinowski M, Honardoost A, Rouf Talukder J, Rabiei R, Delfyett P and Fathpour S 2016 Second-harmonic generation in periodically-poled thin film lithium niobate wafer-bonded on silicon (arXiv:1609.09117)
[16] Chiles J, Toroghi S, Rao A, Malinowski M, Camacho-González G F and Fathpour S 2016 Second-harmonic generation in single-mode integrated waveguides through mode-shape modulation (arXiv:1610.02111)
[17] Rabiei P, Rao A, Chiles J, Ma J and Fathpour S 2014 Low-loss and high index-contrast tantalum pentoxide microring resonators and grating couplers on silicon substrates *Opt. Lett.* **39** 5379
[18] Rabiei P, Ma J, Khan S, Chiles J and Fathpour S 2013 Submicron optical waveguides and microring resonators fabricated by selective oxidation of tantalum *Opt. Express* **21** 6967–72

[19] Fathpour S 2015 Emerging heterogeneous integrated photonic platforms on silicon *Nanophotonics* **4** 143–64

[20] Soref R A, Emelett S J and Buchwald W R 2006 Silicon waveguided components for the long-wave infrared region *J. Opt. A: Pure Appl. Opt.* **8** 840–8

[21] Soref R 2010 Mid-infrared photonics in silicon and germanium *Nat. Photon.* **4** 495–7

[22] Henniger H and Wilfert O 2010 An introduction to free-space optical communications *Radioengineering* **19** 203–12

[23] Phillips R L and Andrews L C 2005 *Laser Beam Propagation Through Random Media* 2nd edn (Bellingham, WA: SPIE) (https://doi.org/10.1117/3.626196)

[24] Hackwell J A, Warren D W, Bongiovi R P, Hansel S J, Hayhurst T L, Mabry D J, Sivjee M G and Skinner J W 1996 LWIR/MWIR imaging hyperspectral sensor for airborne and ground-based remote sensing *Proc. SPIE* **2819** 102–7

[25] Coddington I, Newbury N and Swann W 2016 Dual-comb spectroscopy *Optica* **3** 414

[26] Eggleton B J, Luther-Davies B and Richardson K 2011 Chalcogenide photonics *Nat. Photon.* **5** 141–8

[27] Chang Y-C, Paeder V, Hvozdara L, Hartmann J-M and Herzig H P 2012 Low-loss germanium strip waveguides on silicon for the mid-infrared *Opt. Lett.* **37** 2883–5

[28] Logan D F, Giguere M, Villeneuve A and Helmy A S 2013 Widely tunable mid-infrared generation via frequency conversion in semiconductor waveguides *Opt. Lett.* **38** 4457–60

[29] Tai Lin P, Singh V, Kimerling L and Agarwal A M 2013 Planar silicon nitride mid-infrared devices *Appl. Phys. Lett.* **102** 251121

[30] Dave U D, Uvin S, Kuyken B, Selvaraja S, Leo F and Roelkens G 2013 Telecom to mid-infrared spanning supercontinuum generation in hydrogenated amorphous silicon waveguides using a thulium doped fiber laser pump source *Opt. Express* **21** 32032–9

[31] Langford A A, Fleet M L, Nelson B P, Lanford W A and Maley N 1992 Infrared absorption strength and hydrogen content of hydrogenated amorphous silicon *Phys. Rev.* B **45** 13367–77

[32] Kuyken B *et al* 2011 Nonlinear properties of and nonlinear processing in hydrogenated amorphous silicon waveguides *Opt. Express* **19** B146

[33] Kitamura R, Pilon L and Jonasz M 2007 Optical constants of silica glass from extreme ultraviolet to far infrared at near room temperature *Appl. Opt.* **46** 8118–33

[34] Liu X, Osgood R M, Vlasov Y A and Green W M J 2010 Mid-infrared optical parametric amplifier using silicon nanophotonic waveguides *Nat. Photon.* **4** 557–60

[35] Liu X, Kuyken B, Roelkens G, Baets R, Osgood R M and Green W M J 2012 Bridging the mid-infrared-to-telecom gap with silicon nanophotonic spectral translation *Nat. Photon.* **6** 667–71

[36] Kuyken B, Verheyen P, Tannouri P, Liu X, Van Campenhout J, Baets R, Green W M J and Roelkens G 2014 Generation of 3.6 $\mu$m radiation and telecom-band amplification by four-wave mixing in a silicon waveguide with normal group velocity dispersion *Opt. Lett.* **39** 1349–52

[37] Lau R K W, Lamont M R E, Griffith A G, Okawachi Y, Lipson M and Gaeta A L 2014 Octave-spanning mid-infrared supercontinuum generation in silicon nanowaveguides *Opt. Lett.* **39** 4518–21

[38] Hattasan N, Gassenq A, Cerutti L, Rodriguez J-B, Tournie E and Roelkens G 2011 Heterogeneous integration of GaInAsSb p-i-n photodiodes on a silicon-on-insulator waveguide circuit *IEEE Photonics Technol. Lett.* **23** 1760–2

[39] Grote R R, Souhan B, Ophir N, Driscoll J B, Bergman K, Bahkru H, Green W M J and Osgood R M 2014 Extrinsic photodiodes for integrated mid-infrared silicon photonics *Optica* **1** 264

[40] Sciuto A, Libertino S, Alessandria A, Coffa S and Coppola G 2003 Design, fabrication, and testing of an integrated Si-based light modulator *J. Lightwave Technol.* **21** 228–35

[41] Chuang R W, Hsu M-T, Chou S-H and Lee Y-J 2011 Silicon Mach–Zehnder waveguide interferometer on silicon-on-silicon (SOS) substrate incorporating the integrated three-terminal field-effect device as an optical signal modulation structure *IEICE Trans. Electron.* **E94–C** 1173–8

[42] Roser M, Clayton S R, de la Houssaye P R and Garcia G A 1992 High-mobility fully depleted thin-film SOS MOSFET's *IEEE Trans. Electron Devices* **39** 2665–6

[43] The history of silicon-on-sapphire, (http://admiral-microwaves.co.uk/pdf/peregrine/History_SOS_73-0020-02.pdf)

[44] Pishchik V, Lytvynov L A and Dobrovinskaya E R 2009 *Sapphire* (New York: Springer) (https://doi.org/10.1007/978-0-387-85695-7)

[45] Baehr-Jones T, Spott A, Ilic R, Spott A, Penkov B, Asher W and Hochberg M 2010 Silicon-on-sapphire integrated waveguides for the mid-infrared *Opt. Express* **18** 12127–35

[46] Spott A, Liu Y, Baehr-Jones T, Ilic R and Hochberg M 2010 Silicon waveguides and ring resonators at 5.5 um *Appl. Phys. Lett.* **97** 213501

[47] Zou Y, Subbaraman H, Chakravarty S, Xu X, Hosseini A, Lai W-C, Wray P and Chen R T 2014 Grating-coupled silicon-on-sapphire integrated slot waveguides operating at mid-infrared wavelengths *Opt. Lett.* **39** 3070

[48] Zou Y, Chakravarty S and Chen R T 2015 Mid-infrared silicon-on-sapphire waveguide coupled photonic crystal microcavities *Appl. Phys. Lett.* **107** 81109

[49] Shankar R, Bulu I and Lončar M 2013 Integrated high-quality factor silicon-on-sapphire ring resonators for the mid-infrared *Appl. Phys. Lett.* **102** 51108

[50] Smith C J, Shankar R, Laderer M, Frish M B, Loncar M and Allen M G 2015 Sensing nitrous oxide with QCL-coupled silicon-on-sapphire ring resonators *Opt. Express* **23** 5491–9

[51] Singh N *et al* 2015 Midinfrared supercontinuum generation from 2 to 6 $\mu$m in a silicon nanowire *Optica* **2** 797

[52] Loncar M, Doll T, Vuckovic J and Scherer A 2000 Design and fabrication of silicon photonic crystal optical waveguides *J. Lightwave Technol.* **18** 1402–11

[53] Corcoran B, Monat C, Grillet C, Moss D J, Eggleton B J, White T P, O'Faolain L and Krauss T F 2009 Green light emission in silicon through slow-light enhanced third-harmonic generation in photonic-crystal waveguides *Nat. Photon.* **3** 206–10

[54] Cheng Z, Chen X, Wong C Y, Xu K and Tsang H K 2012 Mid-infrared suspended membrane waveguide and ring resonator on silicon-on-insulator *IEEE Photonics J.* **4** 1510–9

[55] Cheng Z, Chen X, Wong C Y, Xu K, Fung C K Y, Chen Y M and Tsang H K 2012 Focusing subwavelength grating coupler for mid-infrared suspended membrane waveguide *Opt. Lett.* **37** 1217

[56] Wang X, Cheng Z, Xu K, Tsang H K and Xu J-B 2013 High-responsivity graphene/silicon-heterostructure waveguide photodetectors *Nat. Photon.* **7** 888–91

[57] Xia Y, Qiu C, Zhang X, Gao W, Shu J and Xu Q 2013 Suspended Si ring resonator for mid-IR application *Opt. Lett.* **38** 1122–4

[58] Miller S A, Griffith A G, Yu M, Gaeta A L and Lipson M 2016 Low-loss air-clad suspended silicon platform for mid-infrared photonics *CLEO* vol 1 (Washington, DC: OSA) pp 3–4

[59] Soler Penadés J, Alonso-Ramos C, Khokhar A Z, Nedeljkovic M, Boodhoo L A, Ortega-Moñux A, Molina-Fernández I, Cheben P and Mashanovich G Z 2014 Suspended SOI waveguide with sub-wavelength grating cladding for mid-infrared *Opt. Lett.* **39** 5661

[60] Soler Penadés J *et al* 2016 Suspended silicon mid-infrared waveguide devices with subwavelength grating metamaterial cladding *Opt. Express* **24** 22908
[61] Chang C-M and Solgaard O 2013 Fano resonances in integrated silicon Bragg reflectors for sensing applications *Opt. Express* **21** 27209
[62] Chiles J, Khan S, Ma J and Fathpour S 2013 High-contrast, all-silicon waveguiding platform for ultra-broadband mid-infrared photonics *Appl. Phys. Lett.* **103** 151106
[63] Chiles J and Fathpour S 2016 Single-mode and single-polarization photonics with anchored-membrane waveguides *Opt. Express* **24** 19337
[64] Chiles J and Fathpour S 2016 A reliable approach to membrane photonics: the T-Guide *CLEO* (Washington, DC: OSA) STu4R.3 (https://doi.org/10.1364/CLEO_SI.2016.STu4R.3)
[65] Chiles J and Fathpour S 2016 Demonstration of ultra-broadband single-mode and single-polarization operation in T-Guides *Opt. Lett.* **41** 3836
[66] Chang C-M and Solgaard O 2013 Monolithic silicon waveguides in standard silicon *IEEE Micro* **33** 32–40
[67] Chang C-M and Solgaard O 2013 Double-layer silicon waveguides in standard silicon for 3D photonics *CLEO* (OSA) JTu4A.52 (https://doi.org/10.1364/CLEO_AT.2013.JTu4A.52)
[68] Lin P T, Singh V, Cai Y, Kimerling L C and Agarwal A 2013 Air-clad silicon pedestal structures for broadband mid-infrared microphotonics *Opt. Lett.* **38** 1031
[69] Lin P T, Singh V, Hu J, Richardson K, Musgraves J D, Luzinov I, Hensley J, Kimerling L C and Agarwal A 2013 Chip-scale mid-infrared chemical sensors using air-clad pedestal silicon waveguides *Lab Chip* **13** 2161
[70] Yue Y, Zhang L, Huang H, Beausoleil R G and Willner A E 2012 Silicon-on-nitride waveguide with ultralow dispersion over an octave-spanning mid-infrared wavelength range *IEEE Photonics J.* **4** 126–32
[71] Khan S, Chiles J, Ma J and Fathpour S 2013 Silicon-on-nitride waveguides for mid- and near-infrared integrated photonics *Appl. Phys. Lett.* **102** 121104
[72] Spott A *et al* 2016 Quantum cascade laser on silicon *Optica* **3** 545
[73] Spott A *et al* 2016 Heterogeneously integrated distributed feedback quantum cascade lasers on silicon *Photonics* **3** 35
[74] Nedeljkovic M, Soref R and Mashanovich G Z 2011 Free-carrier electrorefraction and electroabsorption modulation predictions for silicon over the 1–14 $\mu$m infrared wavelength range *IEEE Photonics J.* **3** 1171–80
[75] Chiles J and Fathpour S 2014 Mid-infrared integrated waveguide modulators based on silicon-on-lithium–niobate photonics *Optica* **1** 350
[76] Wooten E L *et al* 2000 A review of lithium niobate modulators for fiber-optic communications systems *IEEE J. Sel. Top. Quantum Electron.* **6** 69–82
[77] Sohler W, Grundkotter W, Hofm D, Kostjucenko I, Oriov S, Quiring V, Ricken R, Schreiber G and Suche H 2005 Integrated optical parametric oscillators with Ti:PPLN waveguides *CLEO* vol 1 (Piscataway, NJ: IEEE) pp 195–7
[78] Chen Y, Lin H, Hu J and Li M 2014 Heterogeneously integrated silicon photonics for the mid-infrared and spectroscopic sensing *ACS Nano* **8** 6955–61